

Fuel Resistance of HMAs: Theory and Experiments

Filippo G. Pratico¹⁺, Rachele Ammendola², and Antonino Moro³

Abstract: Fuel spillage on pavement during road transportation can cause deaths, great property damages, and a related decrease level of road safety. Therefore, as far as Hot Mix Asphalts (HMAs) are concerned, the choice of asphalt binders and a specific mix design are of paramount importance in disaster mitigation. In the light of above-mentioned facts, a new model for the analysis of the consequences of fuel spillage has been proposed and validated. The main objectives of the model were the expression of the loss mass (percentage) after soaking in the fuel and after brushing. The purposes of the research were to understand system response to changes in properties, to get a sense for which parameters of bituminous mix control its behavior, and finally to help design the experiments and choose mix type. Laboratory evaluation studies indicate that the formalized models seem to be effective in helping to predict the chemical resistance of HMAs.

Key words: Asphalt binder content; Chemical resistance; Fuel; Pavement; Porosity.

Introduction

Hazardous materials (Hazmat), and in particular fuels, are a potential threat to road networks and airports. In fact, spillage (release) and propagation on road and airport infrastructures are related to many classes of risks. Surface friction, bearing properties, and therefore operational speeds, traffic, and safety are greatly affected in the short, middle, and long term. In the light of the above facts, a model has been formalized for the interpretation of soaking and brushing processes in this study. The model has been finally validated.

Basics for a theory

It is well known that when a fuel spillage occurs, HMAs experience progressively damaged. Moreover, the resistance to shear stresses (for example in landing touchdown phases, see Fig. 1) becomes consequently decreased. The standard EN12697-43: 2005 provides a test method for assessing HMA resistance to fuel. Both soaking (i.e. immersion in fuel and therefore extended action of the fuel) and shear (*per* brushing) actions are considered and two indicators (*A* and *B*) are defined (see Fig. 1).

As is well known, *A* is the loss of mass after soaking in fuel: $A = \sum_i A_i/3$, with $i = 1, 2, 3$ (specimens), $A_i = ((m_{1,i} - m_{2,i})/m_{1,i}) \cdot 100$, $m_{1,i}$ = initial dry mass of the *i*-th specimen for soaking in fuel, in grams(g), $m_{2,i}$ = mass of the *i*-th dry test specimen after soaking in fuel, in grams. The parameter *B* introduced in the standard is there defined as the loss of mass after the brush test: where $B = \sum_i B_i/3$, with $i = 1, 2, 3$ (specimens), $B_i = ((m_{2,i} - m_{5,i})/m_{2,i}) \cdot 100$, $m_{2,i}$ = mass of the *i*-th dry test specimen after soaking in fuel, in grams, $m_{5,i}$ =

mass of the *i*-th test specimen after soaking and after 120 s of brushing, in grams. Note that a third indicator, *C*, has been introduced by the authors in order to have a descriptor able to combine the two different actions (soaking & brushing) and probably better representative of post-spillage pavement performance. *C*(%) is defined as the mean value of the loss of mass of the specimens (see Fig. 1), where $C = \sum_i C_i/3$, with $i = 1, 2, 3$ (specimens), $C_i = ((m_{1,i} - m_{5,i})/m_{1,i}) \cdot 100$.

The models described below have been formalized in order to obtain physical-based expressions for the parameters *A*, *B*, and *C*. If a given mass of fuel is poured into a pavement, the starting mass M_0 (control sample or test specimen) decreases due to the loss of aggregates (*AG*) and asphalt binder (B_A), though small quantities (*F*) of fuel can remain entrapped in the specimen:

$$M_d = M_0 - B_A + F - AG \equiv M_0 - \Delta M \quad (1)$$

where M_d is the mass of the dry sample after Hazmat percolation or soaking in the fuel [1, 2], while ΔM stands for $B_A - F + AG$. The (internal) volume exposed to the fuel, V_p , is:

$$V_p = V \cdot n_{eff} = \sum_j \frac{\pi \phi_j^2 l_j}{4} = \sum_j \pi \phi_j l_j \cdot \frac{\phi_j}{4} \quad (2)$$

where *V* is the total volume of the control sample, n_{eff} is the effective porosity, ϕ_j and l_j are the diameter and the length of the *j*-th internal pore.

Based on the literatures reviewed on this topic [1, 3-7], the diameters ϕ_j can range up to 5mm *circa* (c.a.) while, for ϕ_j below 0.05 microns, neither asphalt binder flows nor absorption can take place. The following expression can be derived:

$$V_p = \sum_j \frac{\pi \phi_j^2 l_j}{4} = \frac{\phi^*}{4} \sum_j \pi \phi_j l_j \quad (3)$$

where ϕ^* is a reference diameter of the pores.

The total exposed surface S_{Te} can be expressed as:

$$S_{Te} \equiv S_p + S_e \quad (4)$$

¹ Associate Professor, DIMET Department, Mediterranean University, Reggio Calabria, Italy, 00 39 0965 875230/875247.

² Research Assistant, DIMET Department, Mediterranean University, Reggio Calabria, Italy, 00 39 0965 875405/875247.

³ Research Assistant, DIMET Department, Mediterranean University, Reggio Calabria, Italy, 00 39 0965 875405/875247.

⁺ Corresponding Author: E-mail filippo.pratico@unirc.it
Note: Submitted April 10, 2008; Revised June 10, 2008; Accepted June 11, 2008.

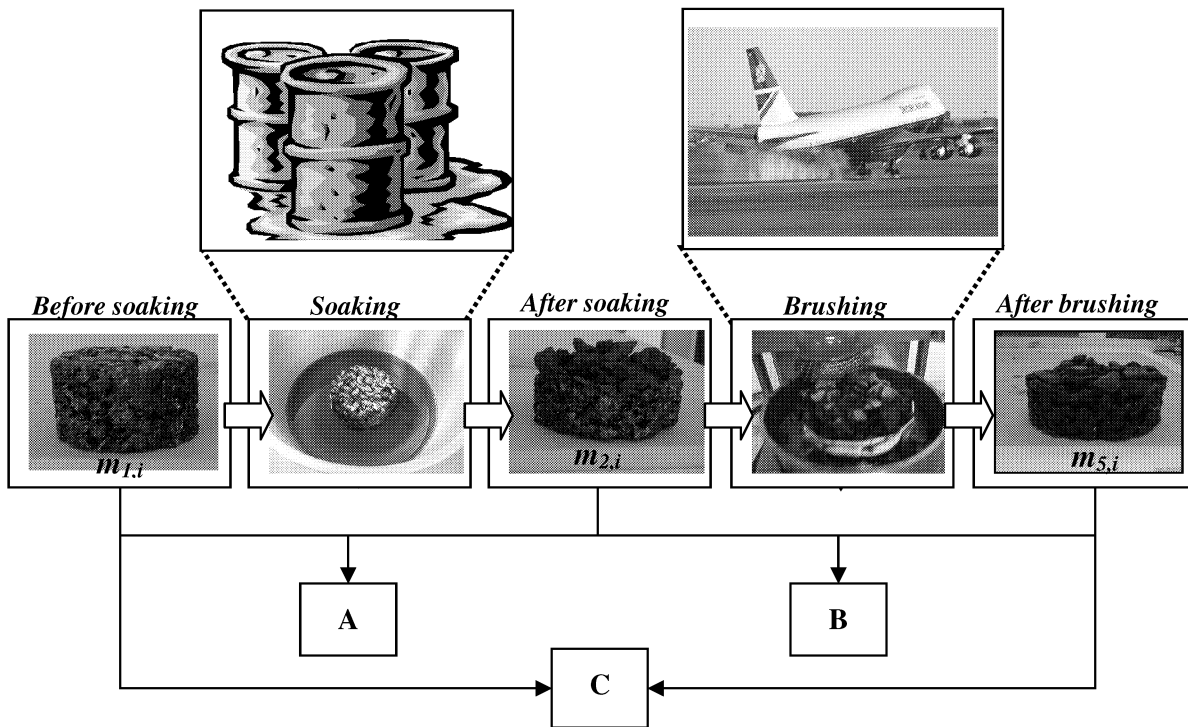


Fig. 1. Fuel Resistance of Hot Mix Asphalts: Specimens, Masses ($m_{j,i}$) and Indicators (A, B, C).

where S_p refers to the (internal) surface of the exposed pores and S_e is the external exposed surface.

By referring to Eqs. (2) and (3), the S_p can be expressed as follows:

$$S_p = \sum_j \pi \phi_j l_j = \frac{4n_{eff} V}{\phi^*} \quad (5)$$

The S_e is defined as follows:

$$S_e = 2\alpha\pi rh + \pi r^2 \quad (6)$$

where r is the radius of the sample and α is a ratio of h_F to h ($0 \leq \alpha \leq 1$); h_F is the height of the fuel around the sample and h is sample height. The coefficient α is negligible for in-site spillage on dense-graded friction courses. Now, suppose that the S_{Te} can be defined as:

$$S_{Te} = a \cdot \frac{\Delta V}{\Delta t} \quad (7)$$

where Δt is the exposition time, ΔV is the volume loss caused by Hazmat percolation into the sample and the parameter a (which has the dimensions of the reciprocal of speed) depends on the particular asphalt binder, size and shape of the flow paths, and fuel characteristics, etc.

From Eqs. (4) to (6), the following expression is derived:

$$\frac{\Delta V}{V} = \frac{\Delta t}{a} \left(\frac{4n_{eff}}{\phi^*} + \left(\frac{2\alpha}{r} + \frac{1}{h} \right) \right) \quad (8)$$

where $V = \pi \cdot r^2 \cdot h$ is the volume of the sample. If i refers to the i -th sample, it is possible to write:

$$\frac{A_i}{100} = \frac{M_{oi} - M_{di}}{M_{oi}} = \frac{\Delta M_i}{M_{oi}} \cong \frac{\Delta V_i \cdot \gamma_L}{V_i \cdot \gamma_{cb}} \quad (9)$$

where γ_L = specific gravity of the loss mass (in practice, γ_L usually ranged from 1g/cm³ c.a up to 3 g/cm³ c.a); γ_{cb} = specific gravity of the specimen. By referring to Eqs. (8) and (9), the following expression is derived:

$$\frac{A_i}{100} = \frac{\Delta M_i}{M_{oi}} = \frac{\Delta V_i \cdot \gamma_L}{V_i \cdot \gamma_{cb}} = \frac{\Delta t}{a} \left(\frac{4n_{eff}}{\phi^*} + \left(\frac{2\alpha}{r} + \frac{1}{h} \right) \right) \cdot \frac{\gamma_L}{\gamma_{cb}} \quad (10)$$

The immersion time Δt is 72hrs \pm 30mins in case a polymer-modified bitumen (PMB) is used, while, if the test is carried out to compare mixtures with paving grade bitumen and PMBs, $\Delta t \approx 24$ hrs \pm 30mins for all specimens. Note that, in the Brush Test on Marshall specimens, α is obtained as

$$\alpha \cong \frac{h_F}{63.5mm} = \frac{35mm}{63.5mm} \cong 0.5 \quad (11)$$

Therefore, in the light of the above formalized model, if a comparison porous-dense mixes (Marshall specimens) is considered, with the same fuel and asphalt binder typologies, it is possible to write (see Eqs. (10) and (11)):

$$\frac{A_i}{100} = \left(\frac{4n_{eff}}{\phi^*} + \frac{2\alpha}{r} + \frac{1}{h} \right) \frac{\Delta t}{a} \cdot \frac{\gamma_L}{\gamma_{cb}} \cong \left[\frac{4n_{eff}}{\phi^*} + E \right] \cdot \frac{G}{\gamma_{cb}} \quad (12)$$

$$\text{where, } E \cong \frac{2 \cdot 0,55 \cdot 2}{10,16cm} + \frac{1}{6,35cm} \cong 0,37cm^{-1}, \quad G \cong \frac{24^h \cdot \gamma_L}{a}$$

Due to the fact that if n_{eff} increases and γ_{cb} decreases, Eq. (12) demonstrates that A has a strong dependence on the effective porosity. Moreover, owing to the presence of the mix specific gravity and the parameter ϕ^* in Eq. (12), it is possible to theorize a dependence on composition parameters and in particular, for ϕ^* , on

the nominal maximum aggregate size, NMAS. As far as the parameter a (introduced by the authors) is concerned, further research is needed for a in many issues. As first attempt, parameter a is assumed as

$$a = -\log \frac{pen_{pre}}{pen_{post}} \quad (13)$$

where pen_{post} is the penetration (0.1mm) on the mix “fuel + asphalt binder”, after 24hrs at 25°C and pen_{pre} is the penetration (0.1mm) on the pure asphalt binder (without fuel), at 25°C. Note that pen_{post} is expected to be greater than pen_{pre} . Moreover, if mixes with same asphalt binder grade are considered, due to dependence of the solvent power of many petroleum products on density (see also [2, 3]), another hypothesis is to consider that the action of the fuel depends on its content of hydrogen and carbonium and therefore on the density of the fuel:

$$a = \alpha_1 \cdot \gamma^{\alpha_2} \quad (14)$$

Another possibility is to consider that the weakening power of the fuel depends on the difference between the density of the water (γ_w) and the fuel (γ):

$$a = (\gamma_w - \gamma)^{\alpha_3} \quad (15)$$

In the light of the above facts, it results:

$$A = (a_1 + b_1 n_{eff}) \cdot (\gamma_w - \gamma)^{\alpha_3} \quad (16)$$

where $\alpha_1, \alpha_2, \alpha_3, a_1, b_1$ are positive coefficients.

As for B , it is possible to observe that the mass of the sample before brush test (M_d) (after Hazmat percolation - soaking in the fuel) is:

$$M_d = h_d \cdot \pi \cdot r^2 \cdot G_{mbdim} \cdot \gamma_w \quad (17)$$

where: h_d = sample height before brush test; G_{mbdim} = bulk specific gravity (dimensional method); γ_w = water density; $A_S = \pi \cdot r^2$ (area of the sample); r = radius of the sample.

The mass of the sample after brush test, $M_b \leq M_d$, is:

$$M_b = h_b \cdot \pi \cdot r^2 \cdot G_{mbdim} \cdot \gamma_w \quad (18)$$

h_b is the sample height after brush test and is defined as:

$$h_b = h_d - \Delta h = h_d \left(1 - \frac{\Delta h}{h_d} \right) \quad (19)$$

Then,

$$\frac{\Delta M}{M} = \frac{(A_S \cdot h_d - A_S \cdot h_b)}{A \cdot h_d} = \frac{\Delta h}{h} \quad (20)$$

where ΔM is mass loss (positive, g), Δh is the height loss (positive, cm). Now, Eq. (20) can be written as

$$\frac{\Delta h}{h} = \frac{\Delta M}{M} = F_L \cdot F_W \cdot F_S \quad (21)$$

F_L, F_W , and F_S are three tentative factors and they are dimensionless. F_L refers to loads and duration and is expressed as:

$$F_L = \Delta t_B \cdot f_L \quad (22)$$

Δt_B is the total brushing time (for example, 120s); f_L is a coefficient which depends on dynamic conditions (pressure, speed of rotation, state of the brush).

As is well known, the work (L) during the brushing test can be written as:

$$L = \sum_i p_i A_{S_i} v_i \Delta t_{B_i} \quad (23)$$

where p_i is the i -th pressure, A_{S_i} is the i -th area (upper surface), v_i is the i -th speed, and Δt_{B_i} is the i -th brushing time.

From Eqs. (22) and (23), it is possible to assume that:

$$F_L = L \cdot K_1 \cong \Delta t_B \cdot f_L \quad (24)$$

K_1 is a calibration coefficient. F_W refers to the potential of the fuel to weaken the asphalt binder. It is defined as:

$$F_W = \log \frac{pen_{post}}{pen_{pre}} \quad (25)$$

For mixes all produced with the same asphalt binder grade, the following formula is proposed as:

$$F_W = \beta_1 \cdot \gamma^{-\beta_2} \quad (26)$$

β_1 and β_2 are calibration coefficients. F_S refers to the sensitivity (of the HMA sample) to be weakened and can be expressed as:

$$F_S = K_2 \cdot S_{Te} = K_2 \cdot (S_p + S_e) \quad (27)$$

Also in this case, the surface of the exposed pores, S_p , may be expressed as follows:

$$S_p = \sum_j \pi \phi_j l_j = \frac{4n_{eff}V}{\phi^*} \quad (28)$$

Similarly, the external exposed surface S_e can be expressed again as:

$$S_e = 2\alpha\pi r h + \pi r^2 \quad (29)$$

From the equations (27) and (28) the total exposed surface, S_{Te} , can be expressed as:

$$K_2 \cdot S_{Te} = K_2 \cdot \left(\frac{4n_{eff}V}{\phi^*} + 2\alpha\pi r h + \pi r^2 \right) = a + b \cdot n_{eff} \quad (30)$$

where K_2, a and b are again calibration coefficients.

Therefore, in the light of the above facts, it is possible to write:

$$B = \frac{\Delta M}{M} \cong \Delta t_B \cdot f_L \cdot \left(\log \frac{pen_{post}}{pen_{pre}} \right) \cdot (a + b \cdot n_{eff}) \quad (31)$$

Also in this case, it is possible to hypothesize the following alternative formula:

$$B = (\gamma_w - \gamma)^{\alpha_4} \cdot (a_2 + b_2 n_{eff}) \quad (32)$$

where α_4, a_2 , and b_2 are positive coefficients.

As for the analysis of parameter C , it is important to observe that

Table 1. Factorial Plan (E, F: Load Levels; $\Delta T_1, \Delta T_2$: Soaking Times; B 70/90: Asphalt Binder Grade).

Diesel oil				Jet A1				Avion 100				H ₂ O			
ΔT_1		ΔT_2		ΔT_1		ΔT_2		ΔT_1		ΔT_2		ΔT_1		ΔT_2	
E	F	E	F	E	F	E	F	E	F	E	F	E	F	E	F
B 70/90															
PEM, DGFC, SMA		PEM, DGFC, SMA		PEM, DGFC, SMA		PEM, DGFC, SMA		PEM, DGFC, SMA		PEM, DGFC, SMA		PEM, DGFC, SMA		PEM, DGFC, SMA	

$$C_i = A_i + (m_{2,i}/m_{1,i}) \cdot B_i$$

Due to the above-mentioned hypotheses, it is possible to write:

$$C \cong (a_1 + b_1 n_{eff})(\gamma_w - \gamma)^{\alpha_3} + (a_2 + b_2 n_{eff})(\gamma_w - \gamma)^{\alpha_4} \cong (a_3 + b_3 n_{eff})(\gamma_w - \gamma)^{\alpha_5} \quad (33)$$

where $a_3, b_3,$ and α_5 are positive. Finally it is interesting to observe that for $\Delta t \cong \Delta t_B \cong 0,$ and/or for $pen_{post} \cong pen_{pre},$ and/or for $\gamma \cong \gamma_w,$ the solutions $A \cong B \cong C \cong 0$ can be easily derived (see Eqs. (12), (16), and (31-33)).

Experimental plan

On the basis of problem statement and modeling, in order to pursue the above-mentioned objectives, the following experiments are planned:

1. Volumetric tests. The following parameters are determined: %b = asphalt binder content as a percentage of aggregates (ASTM 6307-05); carbon tetrachloride has been used as solvent; G = aggregate gradation (EN 12697-2: 2008 [8]; ASTM D6913-04 e 1); NMA S = nominal maximum aggregate size; f(%) = filler content ($d \leq 0.075\text{mm}$); s(%) = sand content ($0.075\text{mm} \leq d \leq 2\text{mm}$); γ_g = aggregate apparent specific gravity (AASHTO T-85:2004); G_{mb} = mix bulk specific gravity (ASTM D6752; ASTM D6857); G_{mbAO} = mix bulk specific gravity after opening (ASTM D6752; ASTM D6857); n_{eff} = mix effective porosity (ASTM D6752; ASTM D6857);
2. Brush tests in order to estimate A, B, and C (EN 12697-43:2005), where: A(%) = mean value of the loss of mass after soaking in fuel; B(%) = mean value of the loss of mass after the brush test; C(%) = mean value of the loss of mass of the specimens.

Factorial plan has been organized as in Table 1. Four different fuel types (diesel oil, $\cong 820\text{--}845\text{kg/m}^3$; Jet A1, $\cong 797.6\text{kg/m}^3$; Avion 100, $\cong 720.0\text{kg/m}^3$; Water, $\gamma_w \cong 1000\text{kg/m}^3$), two different soaking times ($\Delta T_1 = 24\text{hrs} \pm 30\text{mins}$; $\Delta T_2 = 72\text{hrs} \pm 30\text{mins}$), two different load levels, P (E = $60 \pm 3\text{N}$; F = $140 \pm 5\text{N}$), three different types of mixes (PEM-Porous European Mix, DGFC-Dense Graded Friction Course, SMA-Stone Mastic Asphalt) have been considered. All the mixes had the same asphalt binder typology (B 70/90, i.e. with a penetration at 25°C between 7mm and 9mm). Note that water is used for “control samples”. All the experiments are carried out on Marshall specimens.

Results

Tables 2 and 3, Figs. 2 to 8, and Eqs. (34) to (53) summarize the results obtained. In Figs. 2 to 5 scatter plots are reported. In the

same plots, regression lines are shown (where Espo. stands for exponential and lineare for linear), while Eqs. (34) to (50) refer to regressions:

$$A = 0.62B \quad (34)$$

$$A = 0.63C - 3.49 \quad (35)$$

$$A = 0.18\Delta T + 7.82 \quad (36)$$

$$A = -1.43P + 21.50 \quad (37)$$

$$A = 1.87n_{eff} - 9.07 \quad (38)$$

$$A = -0.10\gamma + 102.4 \quad (39)$$

$$B = 0.82C - 1.94 \quad (40)$$

$$B = -0.05\Delta T + 22.69 \quad (41)$$

$$B = -2.04P + 30.05 \quad (42)$$

$$B = 2.37n_{eff} - 9.08 \quad (43)$$

$$B = -0.11\gamma + 113.16 \quad (44)$$

$$C = 0.11\Delta T + 24.94 \quad (45)$$

$$C = -3.01P + 42.99 \quad (46)$$

$$C = 3.03n_{eff} - 9.63 \quad (47)$$

$$C = -0.16\gamma + 167.14 \quad (48)$$

$$C = 5 \cdot 10^7 \cdot e^{-0.0182\gamma} \quad (49)$$

$$C = 3 \cdot 10^{45} \cdot \gamma^{-15.219} \quad (50)$$

Note that the theoretical relationships set out above (Eqs. (16), (32), and (33)) agree with Figs. 2 to 5 in which best fits are reported. It is interesting to observe that the structure of the equations for A, B, and C in function of n_{eff} (Eqs. (38), (43), and (47)) is quite stable: a positive coefficient (between 2 and 3) and a negative constant (between -9 and -10, see also Fig. 4). Similarly, this fact is also noticed for the linear relationships that relate A, B, and C to the density of the fuels used (see Eqs. (39), (44), and (48)): a negative coefficient (contained in the range -0.1~-0.2) and a positive constant (102 ~ 167, see also Fig. 5, in which A, B, and C at y-axis with dimensionless are reported in function of $\gamma,$ at x-axis in kg/m^3).

As for the main statistics per mix (see Table 2), it is observed that PEM values (A, B, C) are 3 to 9 times higher than those of DGFC or SMA, while, coefficients of variance are lower for PEMs than for

Table 2. Main Statistics

		PEM	DGFC	SMA
A	\bar{x}	30.93	8.13	3.62
	σ	25.80	8.25	4.16
	$\frac{\sigma}{x} \cdot 100$	83.43	101.48	114.96
B	\bar{x}	40.29	13.51	6.85
	σ	25.29	13.99	7.18
	$\frac{\sigma}{x} \cdot 100$	62.78	103.55	104.90
C	\bar{x}	54.24	18.91	10.81
	σ	29.34	18.19	11.76
	$\frac{\sigma}{x} \cdot 100$	54.09	96.20	108.77

Table 3. R-Square Values and Correlation Significance.

		A	B	C	ΔT	P	n_{eff}	γ
Section 1 : R ² linear	A	1.00	0.84	0.80	0.04	0.01	0.41	0.19
	B	0.84	1.00	0.95	0.00	0.02	0.51	0.16
	C	0.80	0.95	1.00	0.01	0.03	0.53	0.23
	ΔT	0.04	0.00	0.01	1.00	0.00	0.00	0.00
	P	0.01	0.02	0.03	0.00	1.00	0.05	0.00
	n_{eff}	0.41	0.51	0.53	0.00	0.05	1.00	0.00
	γ	0.19	0.16	0.23	0.00	0.00	0.00	1.00
Section 2 : R ² linear and non linear	A	1.00	0.84	0.80	0.04	0.01	0.41	0.19
	B	0.84	1.00	0.98	0.01	0.02	0.51	0.53
	C	0.80	0.98	1.00	0.01	0.03	0.53	0.61
	ΔT	0.04	0.01	0.01	1.00	0.00	0.00	0.00
	P	0.01	0.02	0.03	0.00	1.00	0.05	0.00
	n_{eff}	0.41	0.51	0.53	0.00	0.05	1.00	0.00
	γ	0.19	0.53	0.61	0.00	0.00	0.00	1.00
Section 3 : Correlation Significance	A	-	0.00	0.00	0.00	0.16	0.00	0.00
	B	0.00	-	0.00	0.49	0.07	0.00	0.00
	C	0.00	0.00	-	0.27	0.04	0.00	0.00
	ΔT	0.00	0.49	0.27	-	0.73	0.77	0.85
	P	0.16	0.07	0.04	0.73	-	0.004	0.98
	n_{eff}	0.00	0.00	0.00	0.77	0.00	-	0.56
	γ	0.00	0.00	0.00	0.85	0.98	0.56	-

the remaining mixes. These facts could be related to a prevailing effect of the effective porosity n_{eff} . In fact, R-square values are appreciable for the correlations involving the effective porosity, n_{eff} (see Table 3, in which R-square values are reported). Note that Table 3 is divided into three sections. Section 1 refers to linear R-square values, while in section 2 the best R-square (linear or not) is reported. Finally in the section 3 of Table 3 the level of significance of correlations (p-value) is shown: the smaller the p-value the more significant the result. Each section of Table 3 can be divided into 4 parts. The first part (first three rows \times first three columns) relates to relationships among the selected indicators of fuel resistance (R² ranges from 0.80 up to 0.98).

The second part (first three rows \times last four columns) and the third part (last four rows \times first three columns) are the most interesting because they relate to the selected indicators of fuel resistance (A, B, and C) to the characteristics of the spillage action (ΔT , P, and γ) and to HMA volumetrics (n_{eff}). In practice, soaking time and load level do not affect spillage action for the selected levels. On the contrary, A, B, and C appear to be strongly dependent

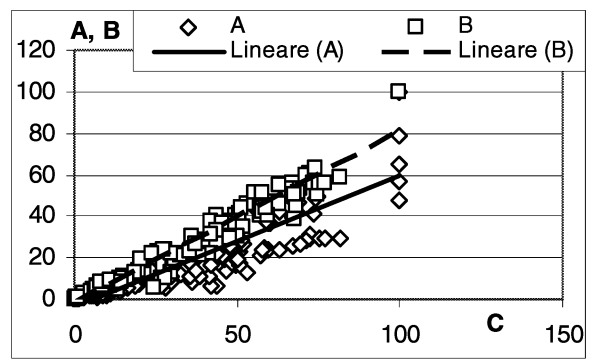


Fig. 2. A, B vs. C

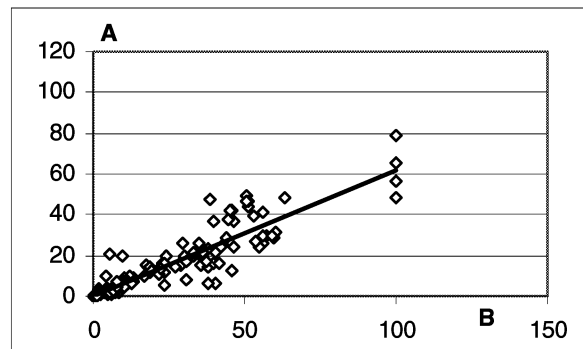


Fig. 3. A vs. B.

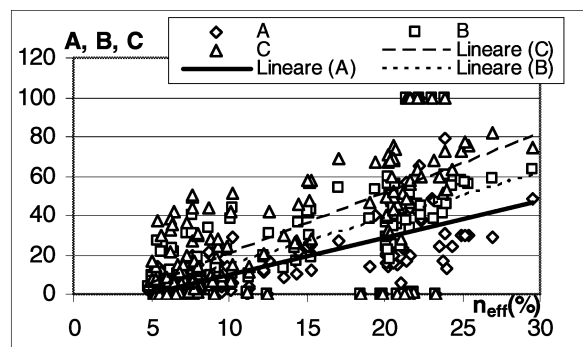


Fig. 4. A, B, and C vs. n_{eff}

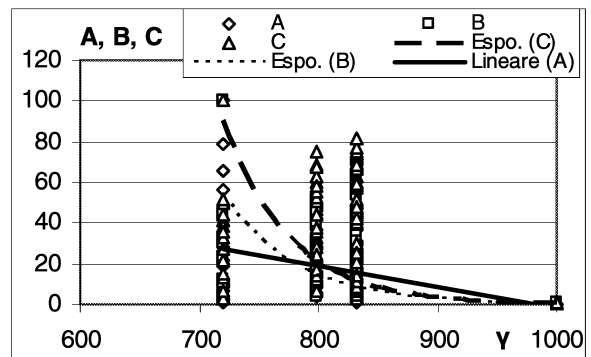


Fig. 5. A, B, and C vs. γ

on the effective porosity (R-square values range from 0.4 up to 0.5) and on fuel density (R-square values range from 0.2 up to 0.6, if non linear relationships are used). The fourth part of the Table 3 (last four rows for last four columns of each section) is not relevant, due

to the fact that such parameters are all independent causes to the mass losses. Constantly in Table 3, (at section 3), it is confirmed that the effective porosity and fuel typology significantly affect *A*, *B*, and *C* and such correlations are statistically valid at a 1% level of significance.

Finally, a regression analysis is carried out in order to assess the relationship between one dependent variable (“effect”: *A*, *B*, or *C*) and several independent variables (“causes”: n_{eff} and γ ; see Eqs. (51) to (53) and scatter plots Figs. 6 to 8).

$$A = (n_{eff} b_1 + a_1) \cdot (\gamma_w - \gamma)^{\alpha_3} \tag{51}$$

$$B = (n_{eff} b_2 + a_2) \cdot (\gamma_w - \gamma)^{\alpha_4} \tag{52}$$

$$C = (n_{eff} b_3 + a_3) \cdot (\gamma_w - \gamma)^{\alpha_5} \tag{53}$$

The resulting R-square values (which range from 0.76 up to 0.82, see Figs. 6 to 8) provide an indication of the goodness of fit of the model, which results appreciable and substantially higher than the ones provided through monivariate correlations (which range from 0.19 up to 0.63 for γ , and from 0.41 to 0.53 for n_{eff} , see Table 3). The following coefficients are obtained:

$$b_1 = 2.24 \cdot 10^{-5}, a_1 = -1.09 \cdot 10^{-4}, \alpha_3 = 2.17, R^2 = 0.81 \text{ (Eq. (51));}$$

$$b_2 = 0.01, a_2 = -0.04, \alpha_4 = 1.00, R^2 = 0.76 \text{ (Eq. (52)); } b_3 = 0.01, a_3 = -0.04, \alpha_5 = 1.04, R^2 = 0.82 \text{ (Eq. (53)).}$$

Note that b_i and a_i are positive as assumed, while a_i are negative (this could be related to the existence of a inferior threshold for n_{eff}). From a practical standpoint, it is important to point out that, as far as EN 12697-43: 2005 is considered, three classes of fuel resistance are defined:

1. good resistance to that fuel ($A \leq 5\%$, $B < 1\%$);
2. moderate resistance to that fuel ($A \leq 5\%$, $1\% \leq B \leq 5\%$);
3. poor resistance to that fuel ($A > 5\%$ or $B > 5\%$).

Now, based on the results obtained, for $n_{eff} \leq 4\%$ (therefore, air voids content $AV \leq 4.4\%$ [3]) a moderate to good resistance to the three considered “true” fuels (diesel oil, Jet A1, Avion 100) can be derived.

Lesson Learned

Many lessons were learned during the three years of implementation of the research program on fuel spillage. Some features were progressively added/changed in the models, and the correlations were continuously refined. Every six months, feedback was taken, and adjustments were made to improve the final outputs. In the light of the results obtained, the following main findings can be drawn. Soaking time, if in the range of 24-72hrs, doesn’t greatly affect on the mass loss of the pavement, neither the consequent tendency to be weakened under shear actions. Similarly, the load between the brush and the specimen, for the levels considered ($60 \pm 3N$ and $140 \pm 5N$), does not appreciably influence on the indicators *B* and *C* which take into account for the resistance to brushing actions.

The effective porosity of the HMA (and, consequently, the air voids content) controls the process of soaking and weakening and it

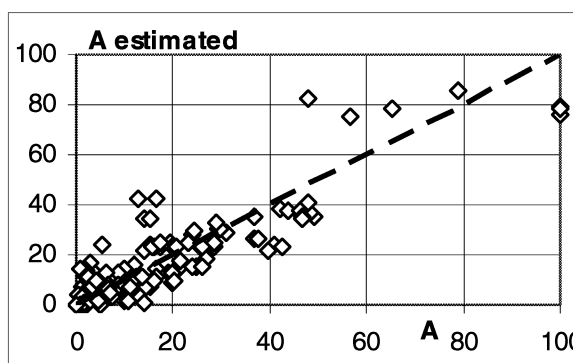


Fig. 6. *A* Estimated vs. *A* ($R^2=0.81$).

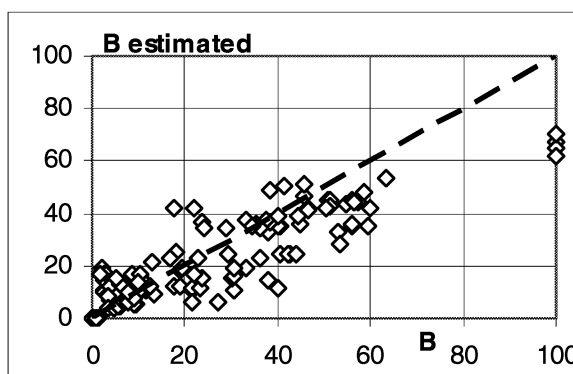


Fig. 7. *B* Estimated vs. *B* ($R^2=0.76$).

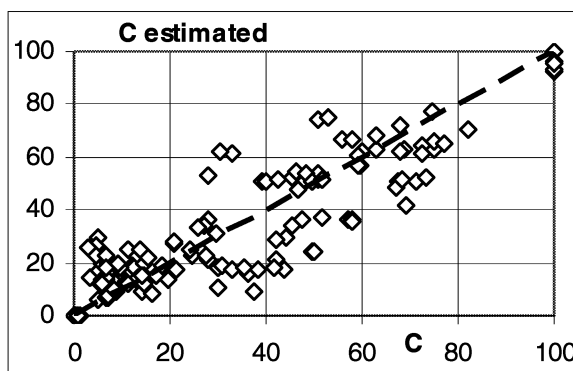


Fig. 8. *C* Estimated vs. *C* ($R^2=0.82$).

is able to explain up to 53% of the process variance. As a consequence, *A*, *B*, and *C* are greatly affected by the effective porosity of the mix and a suitable (and comparatively inexpensive) strategy to reduce the damage caused by fuel spillage is to design very dense mixes (e.g. DGFCs with $AV \leq 4.4\%$ c.a). On the other hand, it is important to remark that the three indicators *A*, *B*, and *C* are well correlated. Fuel density, which is inversely expressive of the deterioration power of the fuel, can explain up to 61% of the process variance. Future research will be aimed at gaining a better understanding of the influence of asphalt binder properties on the effects and how they are related to physical properties of soaked specimens.

References

1. Kandhal, P.S. and Khatri, M.A., (1992). Relating Asphalt

- Absorption to Properties of Asphalt Cement and Aggregates, *NCAT Report No. 92-2, Presented at the Annual Meeting of the Transportation Research Board*, Washington, D.C., USA., pp. 76-84.
2. Praticò, F.G., Ammendola, R., and Moro, A., (2007). Comparing Porous Mixes Performance in Case of Hazmat Spillage, *International Conference: Advanced Characterization of Pavement and Soil Engineering Materials*, Athens, Greece, Vol. 2, pp. 1105-1114.
 3. Praticò, F.G. and Moro, A., (2007). Permeability and Volumetrics of Porous Asphalt Concrete: a Theoretical and Experimental Investigation, *Road Materials and Pavement Design an International Journal*, 8(4), pp. 799-817.
 4. Torres, C., (2004). Probabilistic Analysis of Air Void Structure and Its Relationship to Permeability and Moisture Damage of Hot Mix Asphalt, *Master Thesis*, Texas A&M University, College Station, Texas, USA.
 5. Maarten, M.J.J., Stet, J.A.M., and Molenaar, A.A.A., (2002). Decision Model for the Use of Polymer Modified Binders in Asphalt Concrete for Airfields, *FAA airport technology transfer conference*, Atlantic City, New Jersey, USA, pp. 1-10.
 6. Steernberg, K., Read, J.M., and Seive, A., (2000). Fuel Resistance of Asphalt Pavements, *2nd Eurasphalt & Eurobitume Congress*, Barcelona, Spain, pp.558- 567, book II.
 7. Van Rooijen, R.C., De Bondt, A.H., and Corun, R.L., (2004). Performance Evaluation of Jet Fuel Resistant Polymer – Modified Asphalt for Airport Pavements, *FAA airport technology transfer conference*, Atlantic City, New Jersey, USA, pp. 1-12.
 8. EN 12697-2: 2008, Bituminous mixtures - Test methods for hot mix asphalt - Part 2: Determination of particle size distribution.